

SUPPLEMENTAL MATERIALS

Platelets disseminate extracellular vesicles in lymph in rheumatoid arthritis

Running title: Platelets propagate vesicles in lymph in arthritis

Nicolas Tessandier¹, Imene Melki¹, Nathalie Cloutier¹, Isabelle Allaey¹, Adam Miszta², Sisareuth Tan³, Andreea Milasan⁴, Sara Michel¹, Abderrahim Benmoussa⁵, Tania Lévesque¹, Francine Côté⁶, Steven E. McKenzie⁷, Caroline Gilbert¹, Patrick Provost¹, Alain R. Brisson³, Alisa S. Wolberg², Paul R. Fortin^{1,8}, Catherine Martel⁴ and Éric Boilard^{1,8}.

¹: Centre de recherche du CHU de Québec, Québec, QC, Canada; Département de microbiologie-infectiologie et d'immunologie, Université Laval, Québec, QC, Canada.

²: Department of Pathology and Laboratory Medicine, University of North Carolina, Chapel Hill, NC, USA.

³: Extracellular Vesicles and Membrane Repair, UMR-5248-CBMN CNRS-University of Bordeaux-IPB, Allée Geoffroy Saint-Hilaire, Pessac, France.

⁴: Department of Medicine, Faculty of Medicine, Université de Montréal, Montreal, Quebec, Canada; Montreal Heart Institute, Montreal, Quebec, Canada.

⁵: Department of Nutrition, CHU Sainte-Justine, Université de Montréal, Montreal, Quebec, Canada.

⁶: Institut Imagine, Inserm U1163, Laboratoire Olivier Hermine, Porte 216, 24 blvd Montparnasse, Paris, 75015, France.

⁷: Cardeza Foundation for Hematological Research, Thomas Jefferson University, Philadelphia, PA 19107

⁸ Axe maladies infectieuses et inflammatoires, Centre de recherche du CHU de Québec – Université Laval, Québec, QC, Canada

Correspondence should be sent to: Eric Boilard, PhD

Centre de Recherche du Centre Hospitalier Universitaire de Québec

Faculté de Médecine de l'Université Laval

2705 Laurier Blvd, room T1-49, Québec, QC, Canada G1V 4G2

Eric.Boilard@crchudequebec.ulaval.ca

Phone: +1 418-525-4444, extension 46175, Fax: +1 418-654-2765

Word count: 7500

Keywords: Platelet, Lymph, Inflammation, Vascular permeability

Mice

C57BL/6J (FcγRIIA^{Null} mice), FcγRIIA^{TGN} hemizygous mice were obtained from The Jackson Laboratory. FcγRIIA^{TGN} hemizygous mice described as expressing human FcγRIIA on platelets, megakaryocytes, monocytes, macrophages, neutrophils, eosinophils, basophils, mast cells, and dendritic cells were backcrossed to C57BL/6J for more than ten generations. $\beta_3^{-/-}$ and Tph1^{-/-} mice were crossed with FcγRIIA^{TGN} mice to obtain FcγRIIA^{TGN}:: $\beta_3^{-/-}$ and FcγRIIA^{TGN}::Tph1^{-/-} mice^{19,47-49}. FcγRIIA^{TGN} mice were also crossed with mice expressing red fluorescent protein (RFP) in mitochondria to generate FcγRIIA^{TGN} mice with fluorescent mitochondria, FcγRIIA^{TGN}::Mitochondria-DsRed mice⁵⁰. Guidelines of the Canadian Council on Animal Care were followed in a protocol approved by the Animal Welfare Committee at Laval University (2017122-2). The experiments implicating the examination of the role of β_3 and Tph1 required breeding of FcγRIIA transgenic mice and the respective gene deficient mice. In these conditions where reduced number of mice with the desired genotypes are generated, male and female mice were pooled to achieved sufficient N for further analyses.

Inflammatory arthritis induction in mice

Inflammatory arthritis was induced using arthritogenic K/BxN serum (150 μ L for all experiments, except when specified otherwise), transferred by intra-peritoneal injection to age- and sex-matched FcγRIIA^{Null}, FcγRIIA^{TGN}, FcγRIIA^{TGN}:: $\beta_3^{-/-}$, FcγRIIA^{TGN}::Tph1^{-/-} or FcγRIIA^{TGN}::DsRed mice, on experimental day 0 and 2. The development of arthritis was monitored daily by assessing the clinical index of arthritis, graded on a 0 to 12 scale, as previously described⁵⁷. Delta ankle thickness was measured at the malleoli, with the ankle in a fully-flexed position, using a spring-loaded precision caliper (Käfer dial thickness gauge J15, Germany).

Lymph collection

Mice were fasted for 12h before lymph collection. Mice were anesthetized with isoflurane (2.5% for induction, 2% for maintenance) and placed on their right side, and a cannula was inserted into the thoracic duct, above the cisterna chyli, between the transverse lumbar artery and the diaphragm (Fig. 1a), as previously described³⁷. Thoracic lymph was collected continuously for 45 min, with a syringe coated with EDTA 0.1 M, except for coagulation assays where lymph was collected on 9:1 volume of 3.2% sodium citrate. Thoracic lymph collection yielded a mean of 30-100 μ L of clear, translucent lymph (Fig. 1b). For some experiments, where mentioned, mesenteric lymph was collected at the mesenteric lymph duct level, close to the superior mesenteric artery. Extreme care was taken throughout the collection procedures to ensure minimal blood contamination. Potential blood contamination in unprocessed fresh lymph was verified by quantifying red blood cells (RBC) and platelets, in comparison to unprocessed anticoagulated blood, or centrifuged plasma (twice at 2,500 g for 15 min, to remove all cells). Unprocessed lymph presented a level of RBC equivalent to 0.03% of blood, and a platelet count equivalent to 0.04% of blood, which were both similar to platelet-free centrifuged plasma (Fig. 1c,d). For all experiments involving EVs, lymph

was centrifuged twice at 2,500 g for 15 min, to remove all residual cells, before being frozen at -80°C .

EV quantification

Samples (1 μL lymph) were labeled with 2 $\mu\text{g}/\text{mL}$ of CD41-BV421 and 1 μM of CellTracker Deep Red for 30 min at room temperature in 100 μL phosphate-buffered saline (PBS), and diluted to 500 μL with PBS before flow cytometry analysis using BD Canto II Special Order Research Product, mounted with a forward scatter coupled to a photomultiplier tube, adapted to small particle quantification. For EV characterization 2 $\mu\text{g}/\text{mL}$ of CLEC-2-PE, CD8-APC, CD45-PerCP-Cy5.5 and podoplanin-PE-Cy7, 5 $\mu\text{g}/\text{mL}$ of CD4-FITC and Gr1-FITC, 1/50 of Annexin V-V450 and 1 μL of Ter119-APC were used. All antibodies and annexin were purchased from BD Biosciences, CA, USA, except for anti-podoplanin and anti-CLEC-2 (Biolegend, CA, USA). PEV were identified as double positive for both CD41 and CellTracker. Before acquisition, a known quantity of fluorescent microspheres (2 μm diameter, Cy5-labeled, Nanocs Inc, NY, USA) was added to each tube. Silica beads were used to determine gates used to exclude events smaller than 100 nm or larger than 1 μm (Kisker BioTech, Germany). Triton 0.05% was used to establish EV labeling specificity given the detergent sensitivity of EV.

Western blot

Lymph was centrifuged twice at 2,500 g for 15 min, to remove all residual cells. Platelet-free lymph (PFL) from Fc γ R1IA^{TGN} control and K/BxN mice were lysed in sample buffer and equivalent volumes were loaded in all lanes. Anti-CD41 antibody was diluted 1:1000 in TBS-T 1% milk and incubated for 2 h at RT. Anti-tumor susceptibility gene 101 (TSG-101) was diluted 1:666 in TBS-T 1% milk and incubated overnight at 4°C . Anti-CD41 and anti-TSG-101 antibodies were purchased from Abcam (Cambridge, United Kingdom).

MicroRNA analysis

Fc γ R1IA^{TGN} control and K/BxN lymph were centrifuged twice at 2,500 g for 15 min, to remove all residual cells, before being frozen. RNA was extracted using TRIzol LS Reagent, according to the manufacturer's instructions (ThermoFisher Scientific, MA, USA). Equal amounts of lymph total RNA, extracted from 3 control and 3 K/BxN mice were respectively pooled together. MicroRNA sequencing library preparation and sequencing were conducted by Arraystar, Inc (Rockville, MA, USA). The libraries were denatured as single-stranded DNA molecules, captured on Illumina flow cells, amplified in situ as clusters and finally sequenced for 51 cycles on Illumina HiSeq per the manufacturer's instructions. The clean reads that passed the quality filter were processed to remove the adaptor sequence as the trimmed reads. Trimmed reads were aligned to pre-microRNA in miRBase. MicroRNA read counts were normalized as tag counts per million microRNA alignments (TPM). MicroRNA were ranked by highest TPM, and expressed as a percentage over total read counts per sample. For analysis of PEV microRNA content, CD41⁺ PEV were immunoprecipitated using anti-CD41 coupled magnetic beads (Dynabeads Magnetic Separation Technology, ThermoFisher Scientific,

MA, USA). RNA was extracted using TRIzol LS Reagent. For each RNA extractions, an exogenous synthetic control microRNA (*Caenorhabditis elegans* let-7-as mutated) was spiked-in at the TRIzol-LS homogenization step, as described previously⁵². Total RNA was reverse transcribed using the HiFlex miScript RTII kit (Qiagen), and mature mmu-miR-223 and mature mmu-miR-451 were detected by SYBR Green (SsoAdvanced Universal SYBR Green Supermix, BioRad, CA, USA) qPCR, using the miScript Primer Assay kit (Qiagen) and oligonucleotides specific to mmu-miR-223 (5'UGUCAGUUUGUCAAAUACCCCA; Qiagen) and mmu-miR-451 (5'AAACCGUUACCAUUACUGAGUU; Qiagen). The synthetic let-7-as mutated microRNA was used as a qPCR internal control to calculate the efficiency of microRNA extraction. For pathway analysis, the thirty most frequent microRNAs in control or K/BxN lymph were selected, and their targets were predicted using the multiMiR R package⁵³, with the DIANA-microT database⁵⁴. Top 10 pathways potentially affected by the identified target genes were obtained using the clusterProfiler⁵⁵ R package and the KEGG Pathway⁵⁶ enrichment tool.

Cell screening

Samples (10 μ L total lymph) were incubated with 2 μ g/mL of the following antibodies: anti-mouse-CD8a-V500, anti-mouse-CD11b-BUV661, anti-mouse-CD11c-AF700, anti-mouse-CD45-PerCP, anti-mouse-B220-PE, anti-mouse-Ly6G-PE-CF594, anti-mouse-NK1.1-BV605 and anti-mouse-CD3e-PECy7, 2.5 μ g/mL of anti-mouse-CD4-FITC and 1 μ L of anti-mouse-Ter119-APC in 100 μ L PBS for 30 min. All antibodies were purchased from BD Biosciences, CA, USA. Samples were diluted to 500 μ L in PBS and analyzed using a BD LSRII cytometer.

Coagulation assay

Lymph was collected and centrifuged twice at 2,500 g for 15 min. Mouse blood was obtained by cardiac puncture in syringe containing 20% acid citrate dextrose (ACD), and blood was diluted by the addition of 35% of Tyrode's buffer, pH 6.5. Platelet-free plasma was prepared by centrifuging twice at 2,500 g for 15 min. CD41 vesicles were immunoprecipitated using anti-CD41 coupled magnetic beads (Dynabeads Magnetic Separation Technology, ThermoFisher scientific, MA, USA) and lymph and plasma were stored at -80°C . Thrombin-generating potential was measured by fluorescence in a 96-well plate by incubating 10 μ L of tissue factor (TF)/phospholipids (1 pM and 4 μ M, final, respectively) with 40 μ L of 1:3 diluted samples for 10 minutes at 37°C . Ten μ L of CaCl_2 mixed with thrombin cleavable fluorogenic substrate (ZGGR-AMC, Diagnostica Stago, Parsippany, NJ) (16.6 mM and 0.416 mM, final, respectively) was automatically dispensed in each well and plates were mixed by shaking for 10 seconds. Fluorescence was detected by a Fluoroskan Ascent fluorometer (Thermo Fischer Scientific, Waltham, MA) at 390/460 nm (excitation/emission). The increase in fluorescence, signifying thrombin generation, was recorded every 20 seconds.

Blood vessel permeability

One microgram of Sky Blue fluorescent microspheres (510 nm) (Spherotech Inc, IL, USA) were injected intravenously into FcγRIIA^{Null}::β₃^{+/+}, FcγRIIA^{TGN}::β₃^{+/+}, FcγRIIA^{TGN}::β₃^{-/-}, FcγRIIA^{TGN}::Tph1^{+/+} and FcγRIIA^{TGN}::Tph1^{-/-} K/BxN mice, on the seventh day of arthritis (peak of disease). Mice were anesthetized with 3 % isoflurane in O₂ during the procedure. Imaging was performed using a fluorescence imaging system, Xenogen IVIS Lumina III LT (PerkinElmer, MA, USA) and images were captured 2 min after the injection. Images were analyzed using Living Image software. Mice were euthanized 45 min after the microsphere injection and inguinal lymph nodes (ILN) were harvested. Sky-Blue fluorescence was quantified in the ILN using an Infinite M1000 fluorescence plate reader (Tecan, Switzerland).

Ankle lymphatic vessel quantification

Hind paws were collected and fixed for 24 h in 4 % paraformaldehyde prior to paraffin embedding. Sections were stained with 0.5 μg anti-Lyve1 per slide (Abcam, Cambridge, England) and mean vessel area, vessel number and total lymphatic vessel area per square millimeter were quantified with Image J.

PEV generation

Human platelets from were obtained from citrated blood of healthy male and female donors, following an Institutional Review Board-approved protocol (Centre de Recherche Hospitalier Universitaire de Québec et de l'Université Laval, B14-08-2108). Blood was centrifuged at 282 g for 10 min at room temperature (RT) and the supernatant was collected and supplemented with 1/5 volume ACD and 10 mM of ethylenediaminetetraacetic acid (EDTA), before centrifugation at 600 g for 5 min at RT. The supernatant was then centrifuged at 1300 g for 5 min at RT, and the pellet was resuspended in 2 mL Tyrode's buffer pH 6.5, before transfer into 13 mL Tyrode's buffer pH 7.4. Platelets were counted with a Cellometer Auto M10 (Nexcelom Bioscience, MA, USA) and diluted to 100 × 10⁶ or 600 × 10⁶ platelets / mL in Tyrode's buffer pH 7.4. Optionally, for association and confocal experiments, platelets were labeled with 1 μM 5-chloromethylfluorescein diacetate (CMFDA, green fluorescent, Life Technologies, CA, USA) for 10 min at RT. 5 mM CaCl₂ was added to platelets before their stimulation with collagen (0.5 μg/mL; Chrono-Par, PA, USA) for 18 or 5 h at RT. Platelet activation was stopped by the addition of 20 mM EDTA. Remnant platelets were removed by centrifugation at 2000 g for 10 min, at RT. Platelet EV were obtained by centrifugation in swinging buckets at 18,000 g for 90 min at 18°C. Pellets containing PEV were resuspended in Tyrode's buffer pH 7.4 with 5 mM calcium. Platelet EV were quantified by flow cytometry, and frozen at -80°C.

PEV and lymphatic endothelial cell co-incubation

Human microvascular endothelial cells from female dermal tissue (HMVEC-dLyAd, Lonza, NJ, USA) were cultured in EGM-2 MV Microvascular Endothelial BulletKit (Lonza, NJ, USA). At confluence, cells were incubated with 2000 PEV per cell. The

supernatants were collected after 3, 6 and 24h after co-incubation. Cells were washed and labelled 30 minutes at RT with an anti-human podoplanin-PE (Angiobio, CA, USA), then analyzed by flow cytometry. For immunofluorescence staining, cells were cultured on poly-L-lysine- (0.01%) coated micro-slides before co-incubation with PEV. Cells were washed and fixed with 2 % paraformaldehyde for 20 min then stained with Hoechst, dilution 1/10000 (Millipore-sigma, Darmstadt, Germany). For cytokines and chemokines quantification, cells were incubated with 500 PEV per cell for 24h and the co-culture supernatant was collected, centrifuged at 400 g for 5 minutes and frozen at -80°C . IL-6 was quantified using an human IL-6 DuoSet ELISA from R&D Systems, MN, USA) according to the manufacturer's instructions.

Cytokine quantification

Lymph was centrifuged twice at 2,500 g for 15 min, to remove all residual cells. Cytokines and chemokines were quantified in PEV - human lymphatic endothelial cells co-culture undiluted supernatant and 1:2 diluted cell-free lymph respectively by human or murine Multiplex Cytokine / Chemokine Array (Eve Technologies, Calgary, Alberta, Canada).

Statistical analysis

To avoid misinterpretations due to changes in laser performance or other confounders through the extended period that lasted this study, we only made comparisons between EV levels in lymph collected and processed the same day, and analyzed the same day on the same instrument. Results are presented as mean \pm SEM. Shapiro-Wilk test was used as a normality test. Samples were not tested for equal variance. Statistical significance between groups was determined with unpaired Student's t test, or Wilcoxon rank-sum test, when applicable. One-way ANOVA followed with a post-hoc Tukey HSD or two-way ANOVA followed with a post-hoc Holm-Šidák were used for multiple comparisons. In experiments where $n=3$ and $n=4$ were used, data must be interpreted accordingly to the limitations inherent to the sample size. All statistical analyses were done using R software⁵¹.

Data sharing statement

MicroRNA sequencing data are available at ArrayExpress under accession number E-MTAB-8171. Data, analytic methods and study materials are available upon reasonable request, please contact: Eric.Boilard@crchudequebec.ulaval.ca

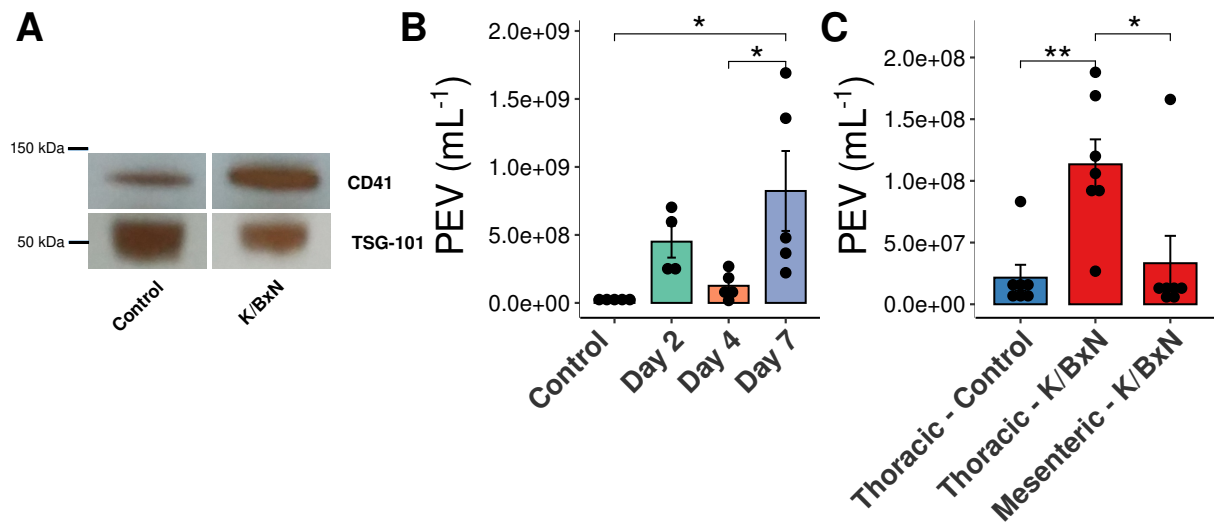
Supplementary References

19. Cloutier N, Allaey I, Marcoux G, et al. Platelets release pathogenic serotonin and return to circulation after immune complex-mediated sequestration. *Proceedings of the National Academy of Sciences of the United States of America*. 2018;115:E1550–E1559.

47. Hodivala-Dilke KM, McHugh KP, Tsakiris DA, Rayburn H, Crowley D, Ullman-Cullere M, Ross FP, Coller BS, Teitelbaum S, Hynes RO. Beta3-integrin-deficient mice are a model for Glanzmann thrombasthenia showing placental defects and reduced survival. *J Clin Invest*. 1999;103:229–238.
48. Zhi H, Rauova L, Hayes V, Gao C, Boylan B, Newman DK, McKenzie SE, Cooley BC, Poncz M, Newman PJ. Cooperative integrin/ITAM signaling in platelets enhances thrombus formation in vitro and in vivo. *Blood*. 2013;121:1858–1867.
49. Côté F, Thévenot E, Fligny C, Fromes Y, Darmon M, Ripoche M-A, Bayard E, Hanoun N, Saurini F, Lechat P, Dandolo L, Hamon M, Mallet J, Vodjdani G. Disruption of the nonneuronal tph1 gene demonstrates the importance of peripheral serotonin in cardiac function. *Proceedings of the National Academy of Sciences of the United States of America*. 2003;100:13525–13530.
50. Hasuwa H, Muro Y, Ikawa M, Kato N, Tsujimoto Y, Okabe M. Transgenic mouse sperm that have green acrosome and red mitochondria allow visualization of sperm and their acrosome reaction in vivo. *Exp Anim*. 2010;59:105–107.
57. Monach P, Hattori K, Huang H, Hyatt E, Morse J, Nguyen L, Ortiz-Lopez A, Wu HJ, Mathis D, Benoist C. The K/BxN mouse model of inflammatory arthritis: theory and practice. *Methods Mol Med*. 2007;136:269–282.
37. Milasan A, Tessandier N, Tan S, Brisson A, Boilard E, Martel C. Extracellular vesicles are present in mouse lymph and their level differs in atherosclerosis. *Journal of extracellular vesicles*. 2016;5:31427.
52. Benmoussa A, Lee CH, Laffont B, Savard P, Laugier J, Boilard E, Gilbert C, Fliss I, Provost P. Commercial Dairy Cow Milk microRNAs Resist Digestion under Simulated Gastrointestinal Tract Conditions. *J Nutr*. 2016;146:2206–2215.
53. Ru Y, Kechris KJ, Tabakoff B, Hoffman P, Radcliffe RA, Bowler R, Mahaffey S, Rossi S, Calin GA, Bemis L, Theodorescu D. The multiMiR R package and database: integration of microRNA-target interactions along with their disease and drug associations. *Nucleic Acids Res*. 2014;42:e133.
54. Paraskevopoulou MD, Georgakilas G, Kostoulas N, Vlachos IS, Vergoulis T, Reczko M, Filippidis C, Dalamagas T, Hatzigeorgiou AG. DIANA-microT web server v5.0: service integration into miRNA functional analysis workflows. *Nucleic Acids Res*. 2013;41:W169–173.
55. Yu G, Wang LG, Han Y, He QY. clusterProfiler: an R package for comparing biological themes among gene clusters. *OMICS*. 2012;16:284–287.
56. Kanehisa M, Sato Y, Kawashima M, Furumichi M, Tanabe M. KEGG as a reference resource for gene and protein annotation. *Nucleic Acids Res*. 2016;44:D457–462.

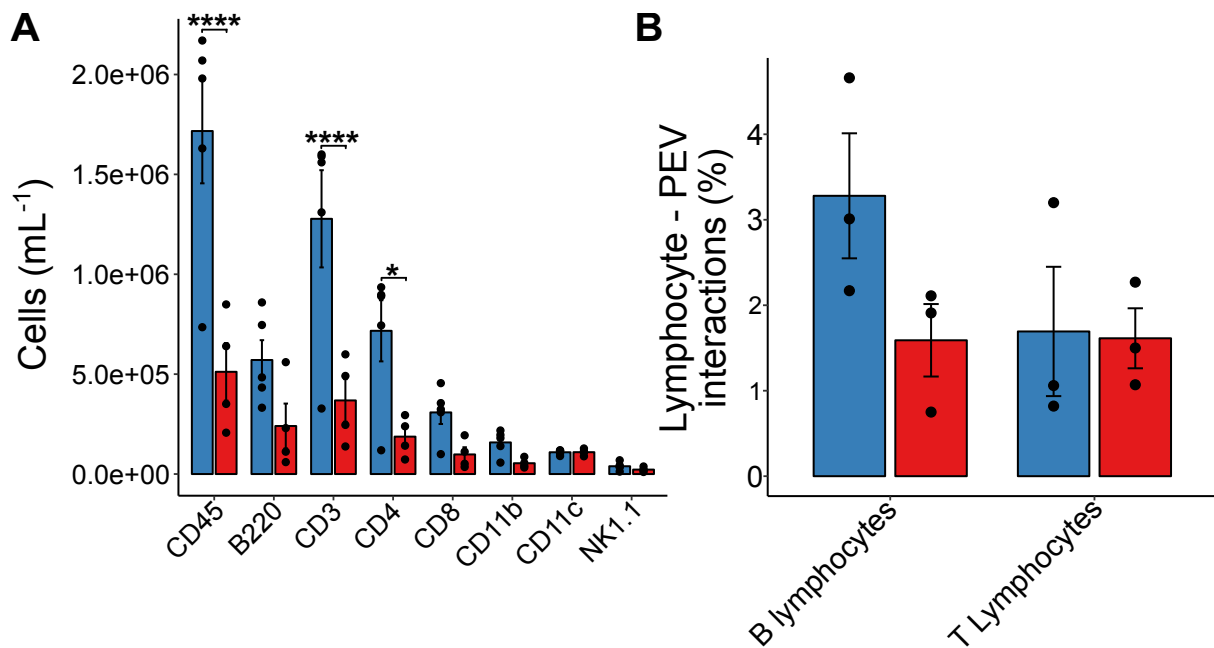
51. R Core Team. R: A language and environment for statistical computing [Internet]. Vienna, Austria: R Foundation for Statistical Computing; 2019. Available from: <http://www.R-project.org/>

Supplementary Figures



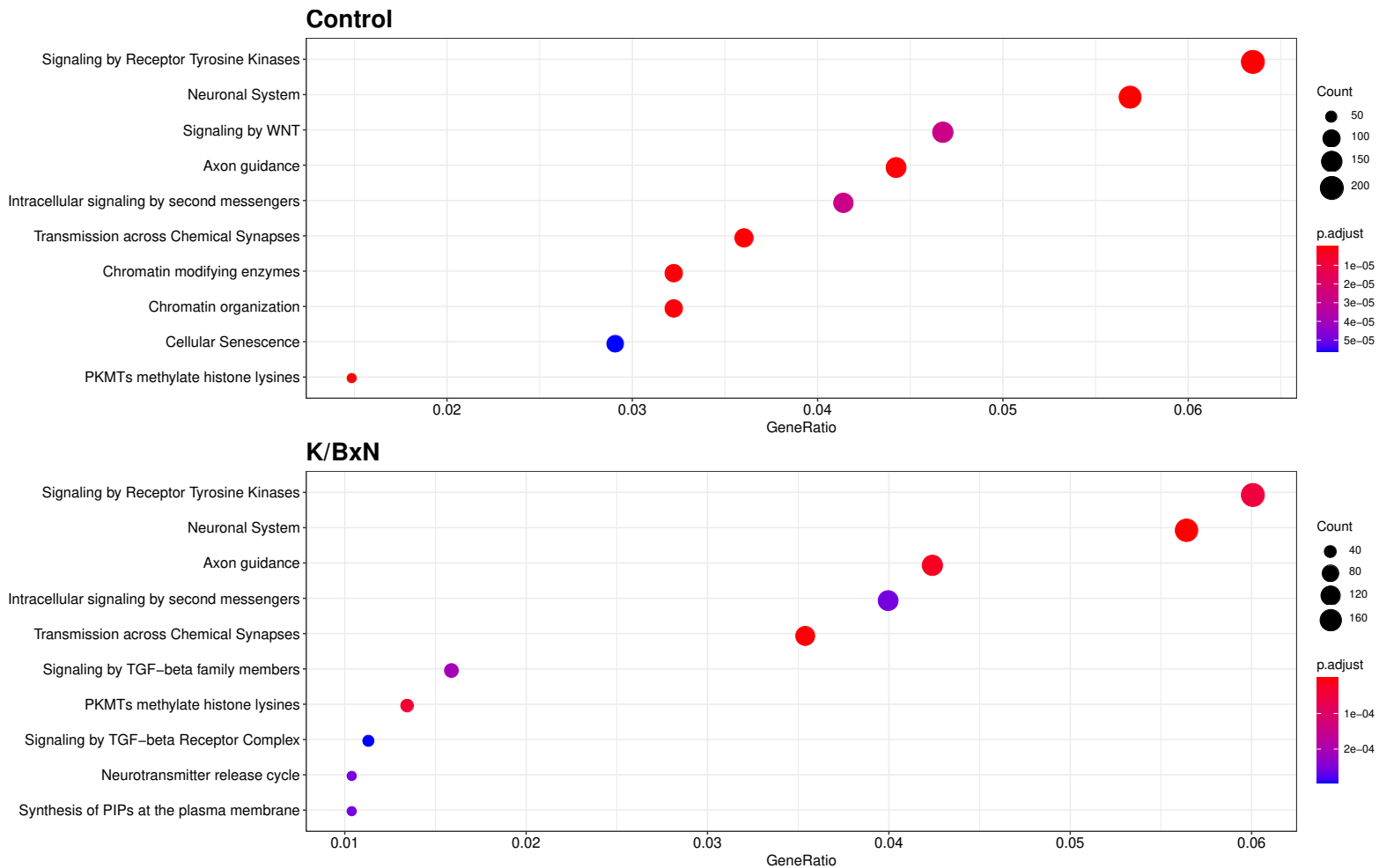
Supplementary Figure I: Characterization of PEV influx in FcγRIIA^{TGN} K/BxN lymph

(A) Platelet-free lymph (PFL) from FcγRIIA^{TGN} control and K/BxN mice were lysed in sample buffer and equivalent volumes were loaded in all lanes. Anti-CD41 antibody was diluted 1 : 1000 in TBS-T 1% milk and incubated for 2 h at RT. Anti-tumor susceptibility gene 101 (TSG-101) was diluted 1 : 100 in TBS-T 1% milk and incubated overnight at 4°C (n=3 (CD41) and n=2 (TSG-101), image representative of 3 experiments (CD41) and 2 experiments (TSG-101)). **(B)** PEV quantification in FcγRIIA^{TGN} K/BxN thoracic lymph, throughout disease progression. Lymph was collected on day 2, day 4 and day 7 following K/BxN serum injection (n=4 (Day 2) or n=5). **(C)** PEV were quantified in thoracic lymph and mesenteric lymph on day 7 after K/BxN serum injection. (n=7). Blue denotes control mice, whereas red identifies K/BxN mice. *: p ≤ 0.05 and **: p ≤ 0.01 using a one-way ANOVA, followed by post-hoc Tukey HSD for multiple comparisons (I and J).



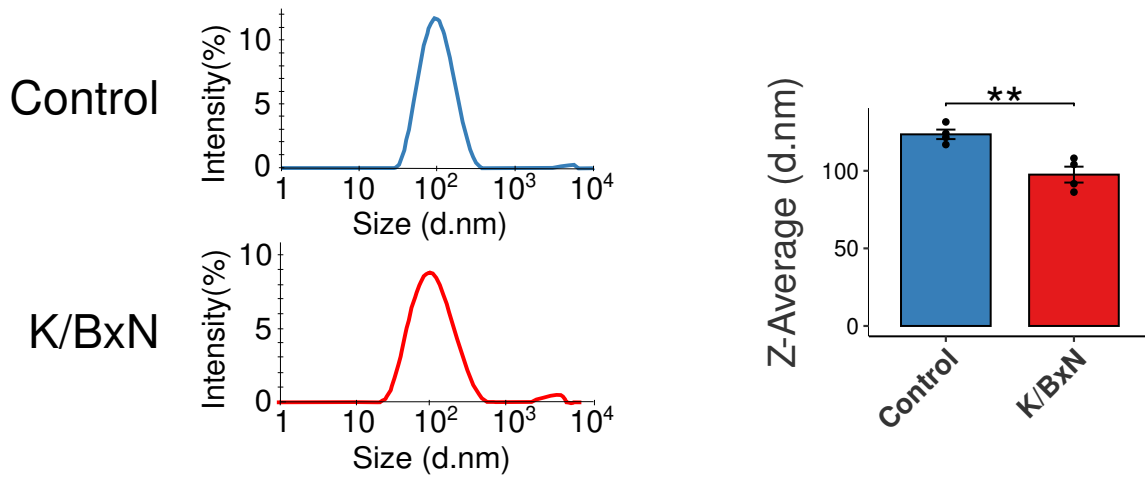
Supplementary Figure II: Cellular characterization of control and K/BxN lymph

(A) Cellular diversity was assessed by flow-cytometry to quantify several immune cell populations in lymph from control and K/BxN lymph at day 7 after K/BxN serum injection in $Fc\gamma RIIA^{TGN}$ mice ($n=5$ control and $n=4$ K/BxN). **(B)** Percentage of PEV associated with circulating B- and T-lymphocytes in lymph ($n=3$). Blue denotes control mice, whereas red identifies RA mice. *: $p \leq 0.05$ and ****: $p \leq 0.0001$ using a two-way ANOVA, followed by post-hoc Holm-Šidák for multiple comparisons.



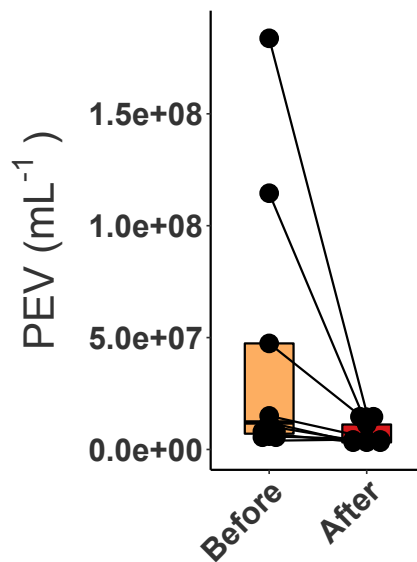
Supplementary Figure III: Pathways potentially impacted by the thirty most frequent micro-RNAs in $Fc\gamma RIIA^{TGN}$ control and K/BxN lymph

Illustration of the 10 pathways most probably impacted by the thirty most frequent micro-RNAs in $Fc\gamma RIIA^{TGN}$ control and K/BxN lymph. Micro-RNAs genes targets were predicted with DIANA-microT and pathways were identified by KEGG PATHWAY (n=3 mice, pooled together into one sample for miR sequencing). GeneRatio identifies the ratio of genes predicted to be targeted by the top 30 lymph micro-RNAs over all the genes forming the pathway.



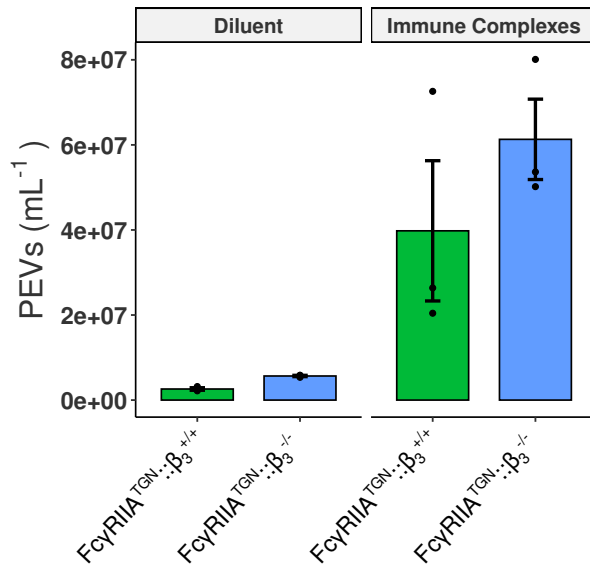
Supplementary Figure IV: Lymph EV diameter analysis

Analysis of lymph EV population diameter was assessed by zetasizer. Representative distribution of EV population in control and K/BxN lymph identifies a major peak at 100 nm of diameter (left). Quantification of mean diameter of main EV population for control and K/BxN lymph (right) (n=4). **: $p \leq 0.01$, using an unpaired t-test.



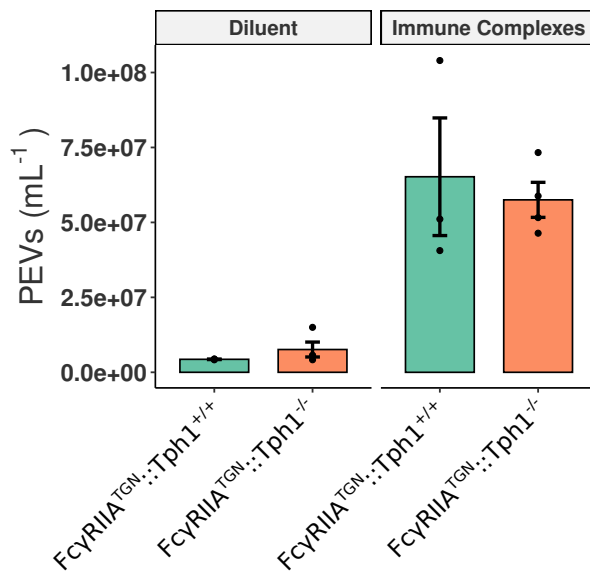
Supplementary Figure V: Assessment of PEV depletion in thrombin generation assay

Thoracic lymph from $\text{Fc}\gamma\text{RIIA}^{\text{TGN}}$ control and K/BxN mice was collected. CD41^+ PEV were depleted using magnetic beads coupled with anti- CD41 antibodies. PEV were quantified before (Before) and after (After) CD41^+ depletion (n=8)



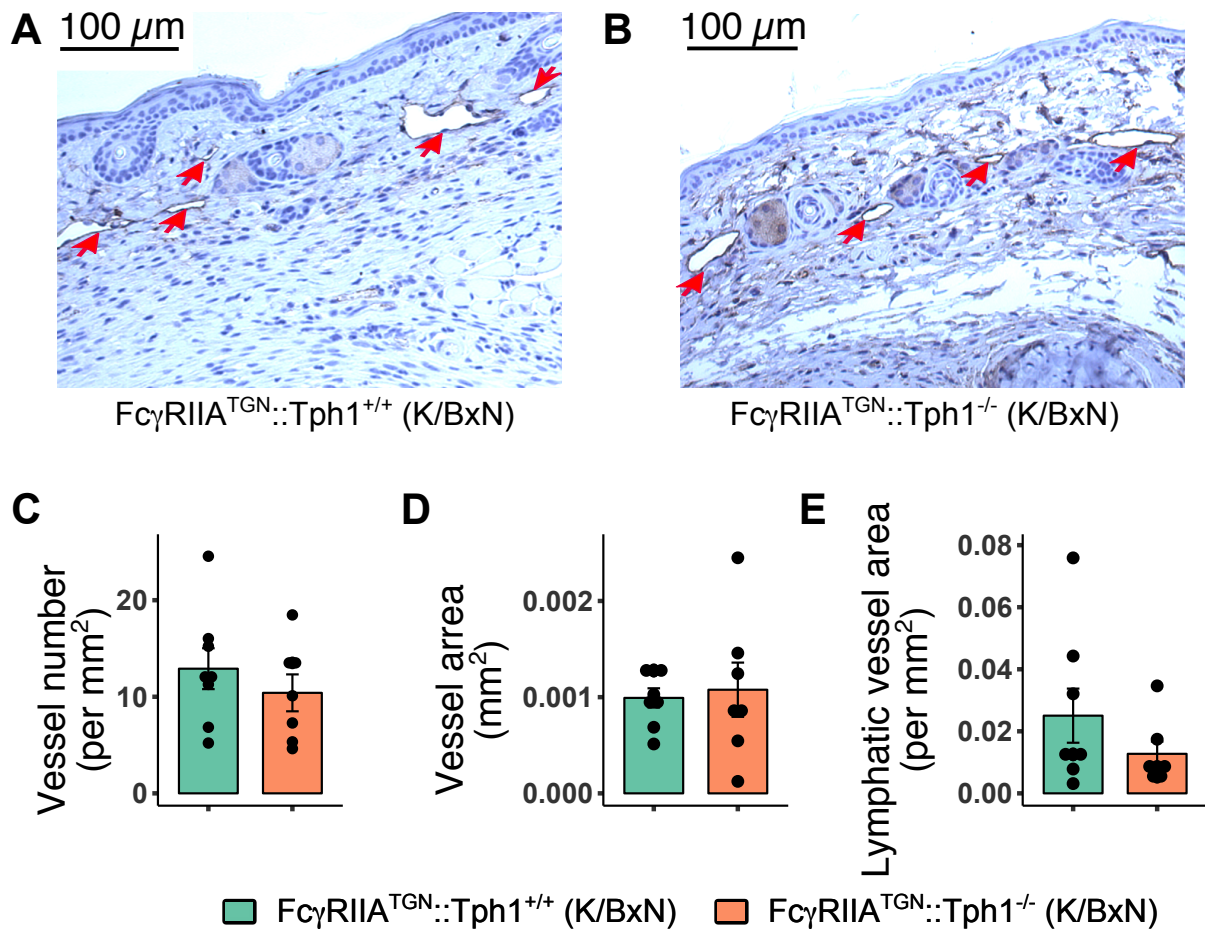
Supplementary Figure VI: The potential of FcγRIIA^{TGN::β3} platelets to generate PEV upon immune complex stimulation is not hindered

(A) Platelets from FcγRIIA^{TGN::β3}+/+ and FcγRIIA^{TGN::β3}-/- mice were isolated and diluted to 200 x 10⁶ per mL before stimulation for 45 minutes with PBS (Diluent) or 500 μg/mL of heat-aggregated IgGs (Immune complexes). PEV were quantified by flow cytometry in the supernatant (n=3).



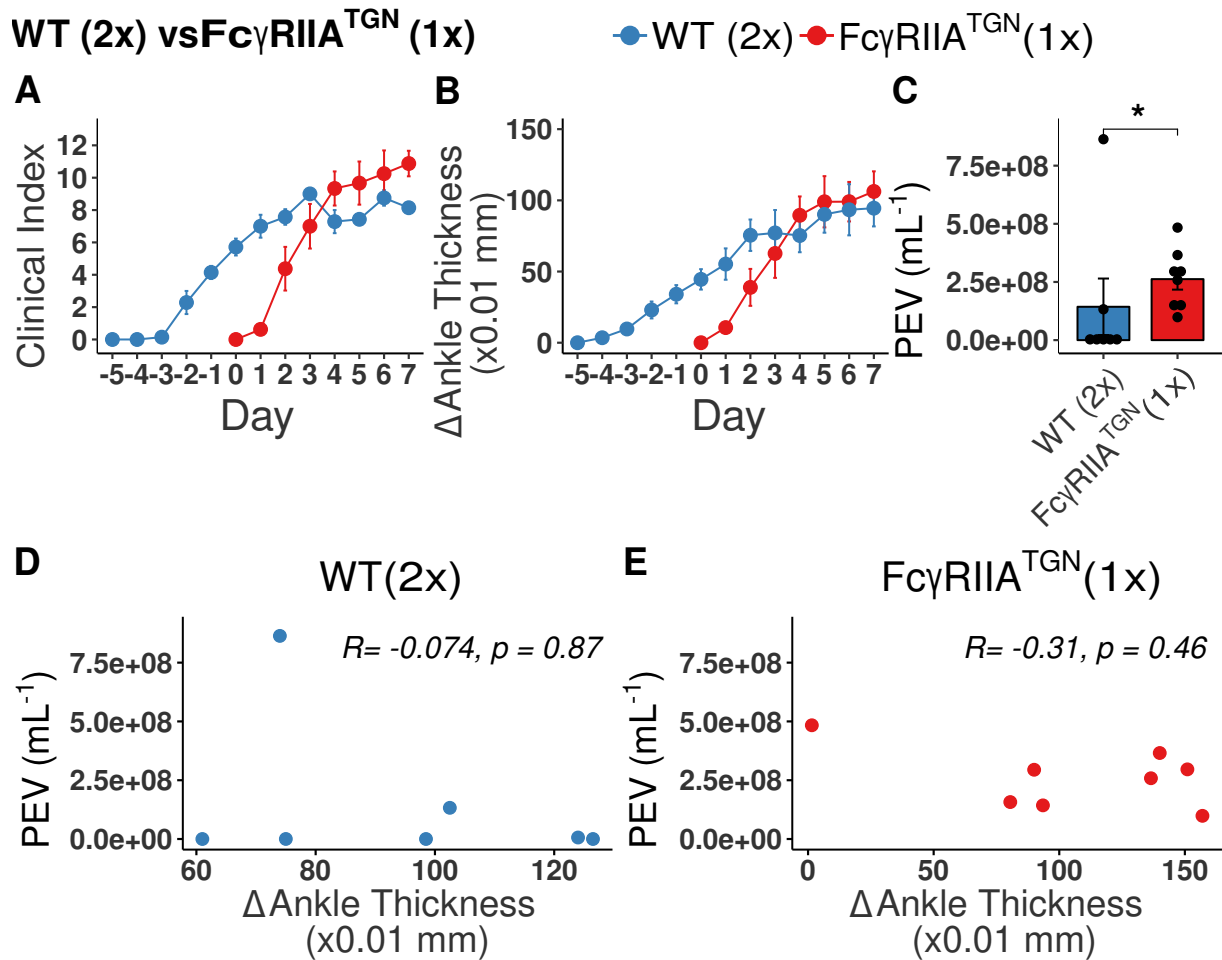
Supplementary Figure VII: The potential of FcγRIIA^{TGN::Tph1} platelets to generate PEV upon immune complex stimulation is not hindered

Platelets from FcγRIIA^{TGN::Tph1}+/+ and FcγRIIA^{TGN::Tph1}-/- mice were isolated and diluted to 200 x 10⁶ per mL before stimulation for 45 minutes with PBS (Diluent) or 500 μg/mL of heat-aggregated IgGs (Immune complexes). PEV were quantified by flow cytometry in the supernatant (n=4 (FcγRIIA^{TGN::Tph1}+/+) and n=3 (FcγRIIA^{TGN::Tph1}-/-)).



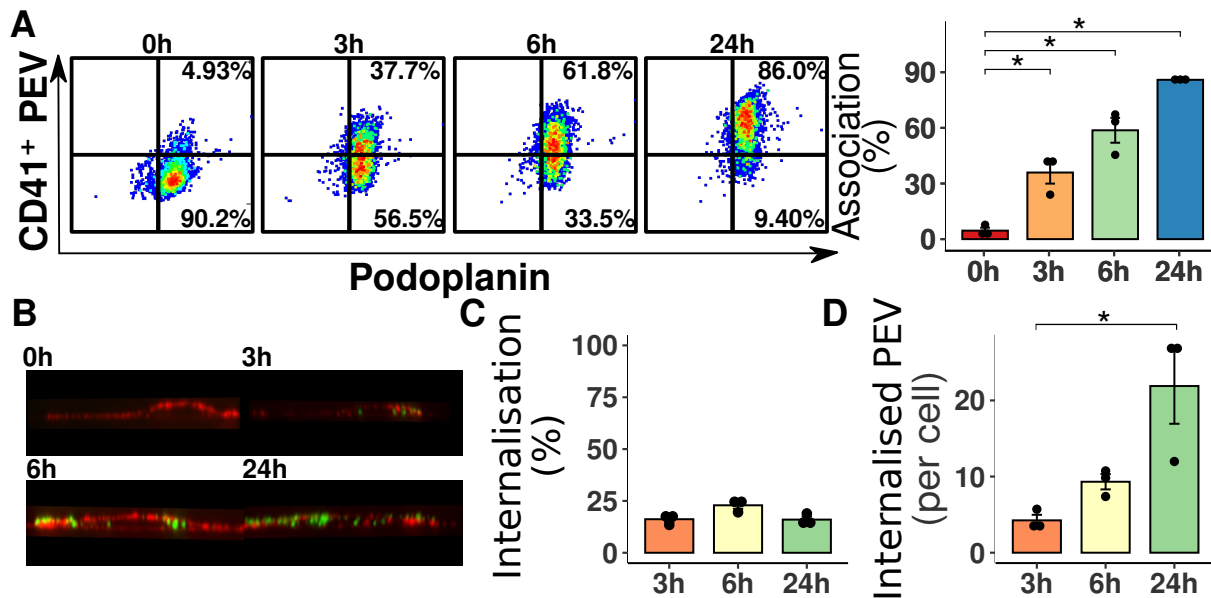
Supplementary Figure VIII: Fc γ RIIA^{TGN::Tph1}^{-/-} mice do not display defective lymphangiogenesis

(A and B) Representative micrographs illustrating lymphatic vessels in the hind paw of Fc γ RIIA^{TGN::Tph1}^{+/+} (A) and Fc γ RIIA^{TGN::Tph1}^{-/-} (B) arthritic mice. Lymphatic vessels were detected with an anti-LYVE-1 antibody. **(C, D and E)** Quantification of the mean lymphatic vessel number per square millimeter of tissue (C), mean lymphatic vessel area (D), and total lymphatic area per square millimeter of tissue in Fc γ RIIA^{TGN::Tph1}^{+/+} and Fc γ RIIA^{TGN::Tph1}^{-/-} arthritic mice (E).



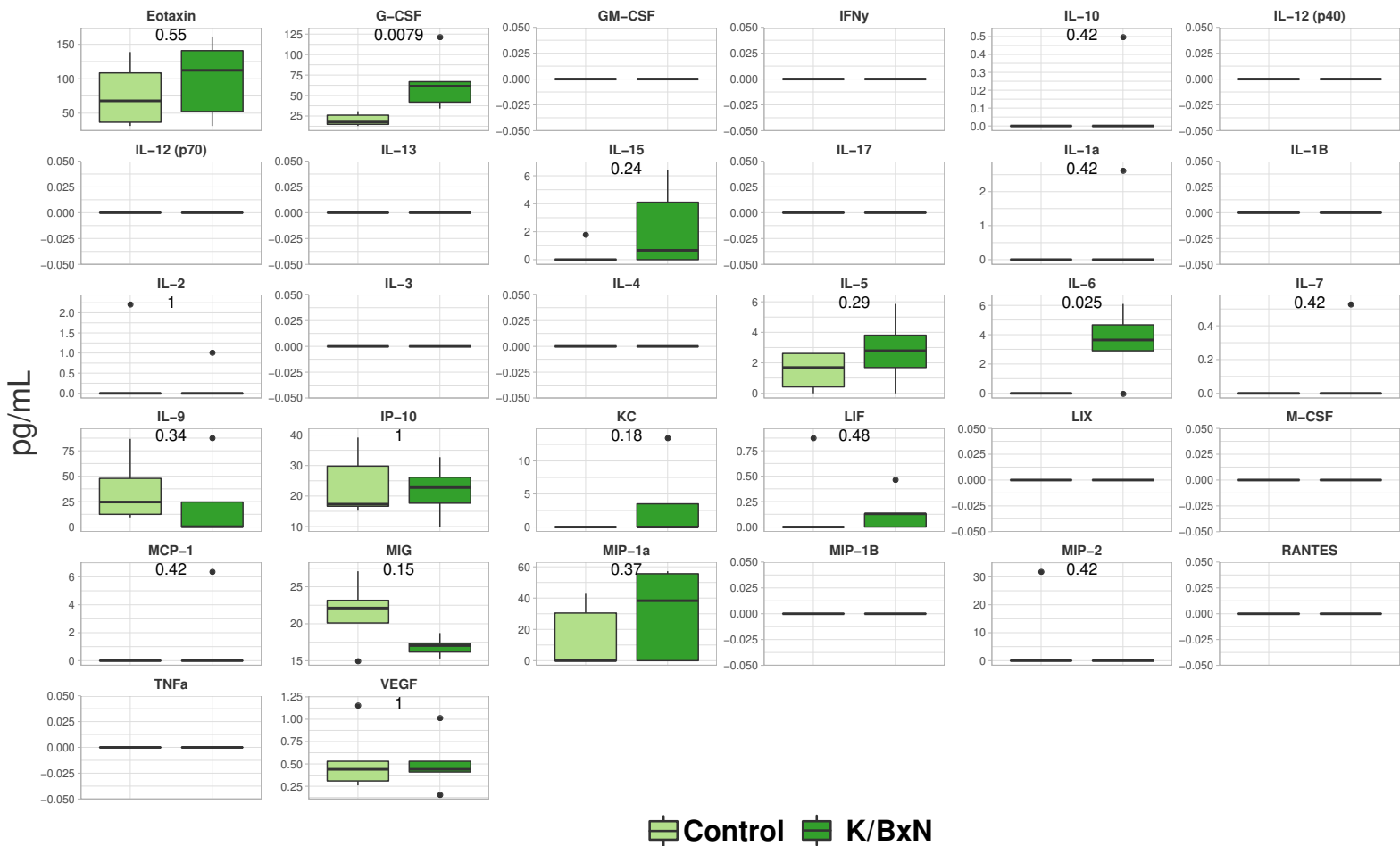
Supplementary Figure IX: Lymph PEV influx in arthritic mice may implicate FcγRIIA expression

(A and B) Clinical index (A) and delta ankle thickness (B) in WT mice injected with 300 μ L K/BxN serum (2x) (blue) on day -5 and day -3 and FcγRIIA^{TGN} mice injected with 150 μ L K/BxN serum (1x) (red) on day 0 and day 2. (n=7) **(C)** Quantification of lymph PEV in WT 2x and FcγRIIA^{TGN} 1x mice at the peak of arthritis severity, day 7. **(D and E)** Spearman correlations of lymph PEV concentration and delta ankle thickness in WT 2x mice **(D)** and FcγRIIA^{TGN} 1x mice **(E)** (n=7 and n=8). *: $p \leq 0.05$, using a Wilcoxon rank-sum test.



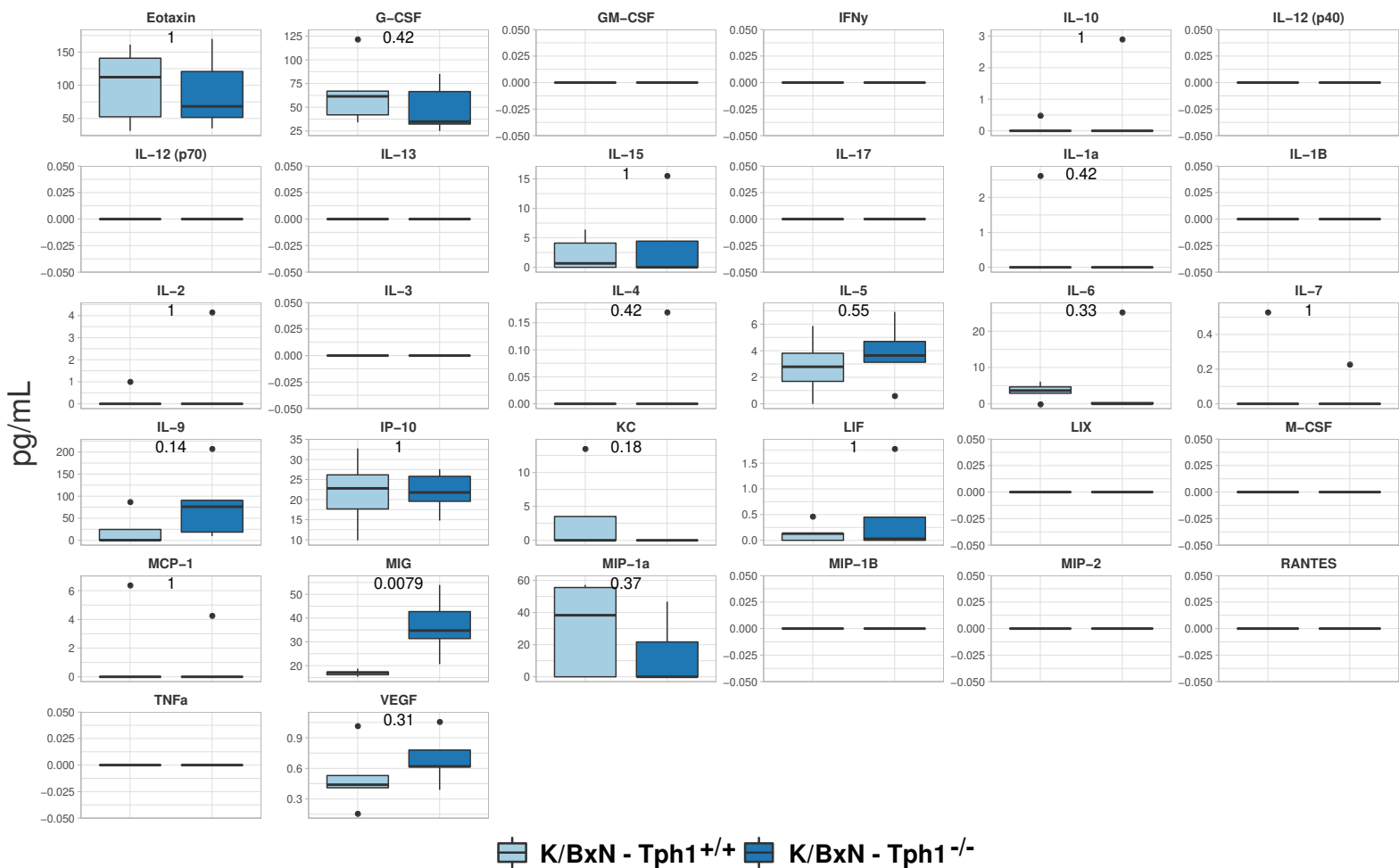
Supplementary Figure X: PEV can be internalised by lymphatic endothelial cells

(A) Representative flow cytometry illustrations of 5-chloromethylfluorescein diacetate- (CMFDA) labeled PEV associating over time with Human Lymphatic Endothelial Cells (hLEC) after co-incubation. Human LEC were washed and labeled with an anti-phycoerythrin-podoplanin antibody. (n=3) (left). Quantification of PEV association with hLEC at 0h, 3h, 6h and 24h post co-incubation (n=3) (right). **(B)** Representative image illustrating PEV internalized by hLECs at 0h, 3h, 6h and 24h post co-incubation. hLECs were 3D-reconstructed with FIJI and visualized as orthoslices with 3D-Viewer plugin. Only yz planes are shown. Red labelling corresponds to wheat germ agglutinin-594, green labeling corresponds to CMTFDA⁺ PEV. **(C and D)** Quantification of PEV internalized by LEC over time for three different PEV donors (n=3, 50 cells per PEV donor). Data are expressed as a percentage of PEV detected in the cytoplasm over PEV bound on the outer leaflet of the membrane (C) or mean PEV number quantified in the cytoplasm of a LEC (D). *: $p \leq 0.05$ using a one-way ANOVA, followed by post-hoc Tukey HSD for multiple comparisons (A and D).



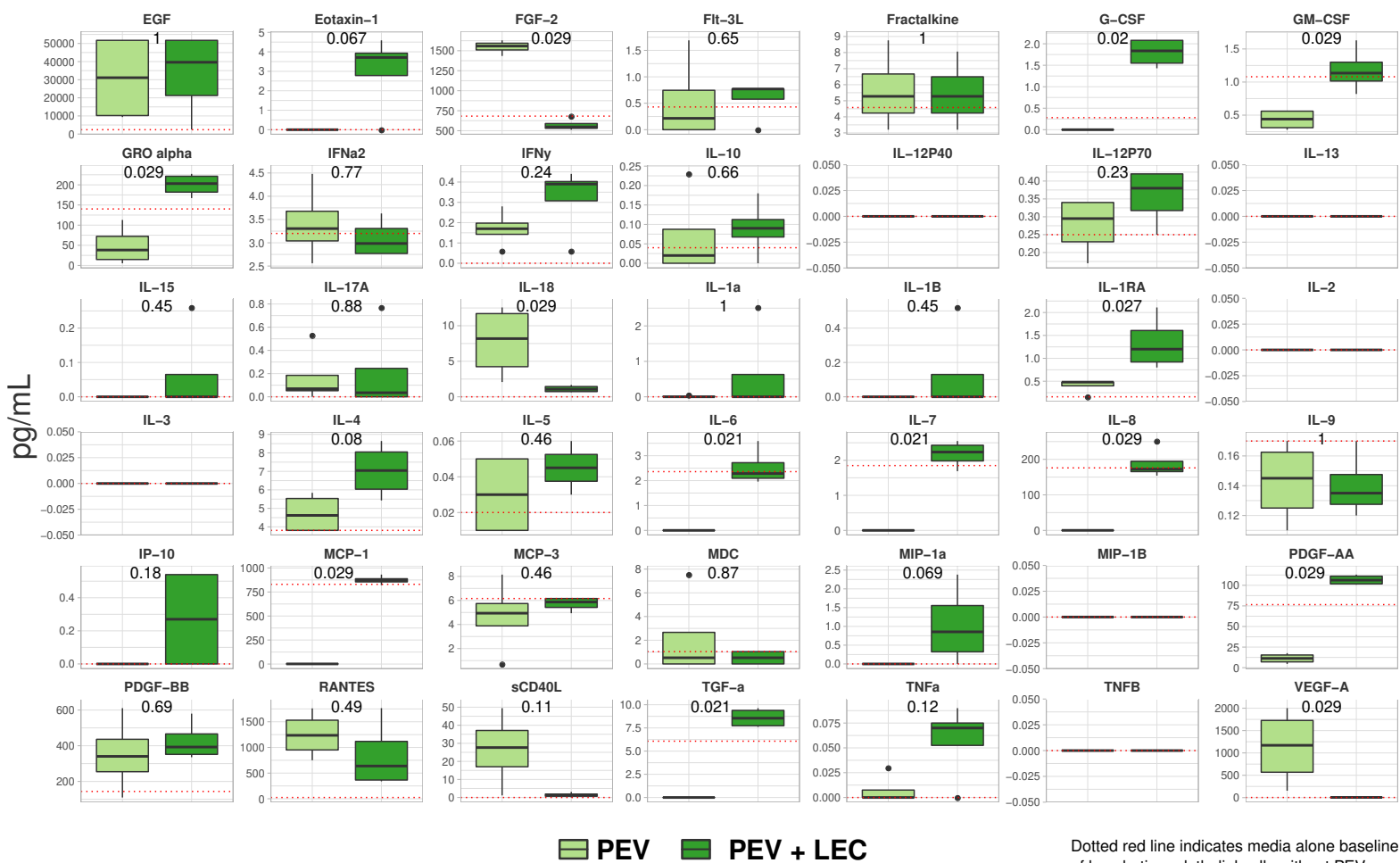
Supplementary Figure XI: Cytokines and chemokines detected in $Fc\gamma RIIA^{TGN}$ control and K/BxN lymph

Quantification of 32 cytokines and chemokines contained in $Fc\gamma RIIA^{Null}$ control and $Fc\gamma RIIA^{TGN}$ K/BxN lymph (n=5). P-value for Wilcoxon rank-sum test is reported on each individual graph.



Supplementary Figure XII: Cytokines and chemokines detected in $Fc\gamma RIIA^{TGN}::Tph1^{+/+}$ and $Fc\gamma RIIA^{TGN}::Tph1^{-/-}$ K/BxN lymph

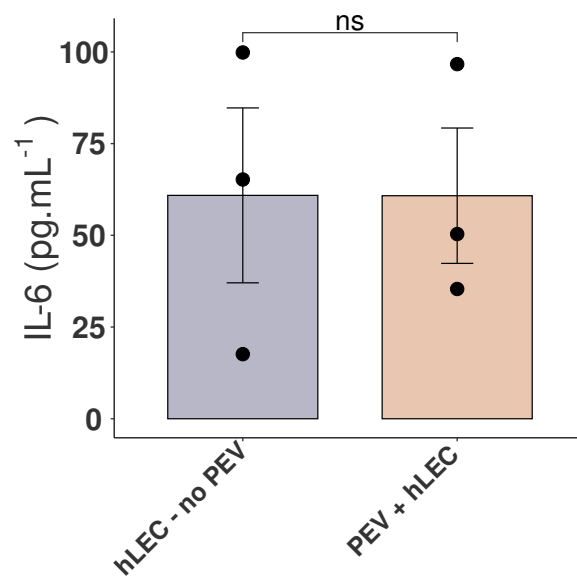
Quantification of 31 cytokines and chemokines contained in $Fc\gamma RIIA^{TGN}::Tph1^{+/+}$ K/BxN and $Fc\gamma RIIA^{TGN}::Tph1^{-/-}$ K/BxN lymph (n=5). The same $Fc\gamma RIIA^{TGN}$ K/BxN mice (n=5) were reported for Fig. SXI and Fig. SXII. P-value for Wilcoxon rank-sum test is reported on each individual graph.



Dotted red line indicates media alone baseline of lymphatic endothelial cells without PEV

Supplementary Figure XIII: Screening of cytokines and chemokines induced upon PEV co-incubation with lymphatic endothelial cells

Quantification of 42 cytokines and chemokines produced upon PEV co-incubation with LEC for 24h. Cytokines and chemokines were quantified by multiplex assay. Dotted red line indicates the media alone baseline production of each analyte (n=4). P-value for Wilcoxon rank-sum test is reported on each individual graph.



Supplementary Figure XIV: Quantification of IL-6 produced upon PEV co-incubation with lymphatic endothelial cells

Quantification of IL-6 produced upon PEV co-incubation with human lymphatic endothelial cells (hLEC) for 24h. IL-6 was quantified by ELISA (n=3 PEV donors and n=3 cell passages). ns: non-significant using an unpaired t-test.

Major Resources Tables

Animals (in vivo studies)

Species	Vendor or Source	Background Strain	Sex
C57BL/6J	The Jackson Laboratory	C57BL/6J	M and F
FcγRIIA ^{TGN}	The Jackson Laboratory	C57BL/6J	M and F
FcγRIIA ^{TGN} ::β ₃ ^{-/-}	Dr Peter Newman's laboratory	C57BL/6J	M and F
FcγRIIA ^{TGN} ::Tph1 ^{-/-}	Dr Francine Côté's laboratory	C57BL/6J	M and F
FcγRIIA ^{TGN} ::Mitochondria-DsRed	Dr. Masaru Okabe's laboratory	C57BL/6J	M and F

Animal breeding

	Species	Vendor or Source	Background Strain	Other Information
Parent - Male	β ₃ ^{-/-}	Dr Peter Newman's laboratory	C57BL/6J	
Parent - Female	FcγRIIA ^{TGN}	The Jackson Laboratory	C57BL/6J	
Parent - Male	Tph1 ^{-/-}	Dr Francine Côté's laboratory	C57BL/6J	
Parent - Female	FcγRIIA ^{TGN}	The Jackson Laboratory	C57BL/6J	
Parent - Male	B6D2F1-Tg(CAG/su9-DsRed2, Acr3-EGFP)RBGS002Osb	Dr. Masaru Okabe's laboratory	C57BL/6J	
Parent - Female	FcγRIIA ^{TGN}	The Jackson Laboratory	C57BL/6J	

Antibodies

Target antigen	Vendor or Source	Catalog #	Working concentration	Lot # (preferred but not required)
CD41-BV421	BD Biosciences	747729	2 µg/mL	
CellTracker Deep Red	Thermofisher Scientific	C34565	1 µM	

CLEC-2-PE	Biolegend	146104	2 µg/mL	
CD8-APC	BD Biosciences	553035	2 µg/mL	
CD45-PerCP-Cy5.5	BD Biosciences	550994	2 µg/mL	
podoplanin-PE-Cy7	Biolegend	127412	2 µg/mL	
CD4-FITC	BD Biosciences	561835	5 µg/mL	
Gr1-FITC	BD Biosciences	553127	5 µg/mL	
Annexin-V450	BD Biosciences	560506	1/50	
Ter119-APC	BD Biosciences	557909	1/50	
CD8a-V500,	BD Biosciences	560776	2 µg/mL	
CD11b-BUV661	BD Biosciences	565080	2 µg/mL	
CD11c-AF700	BD Biosciences	560583	2 µg/mL	
B220-PE	BD Biosciences	553089	2 µg/mL	
Ly6G-PE-CF594	BD Biosciences	562700	2 µg/mL	
NK1.1-BV605	BD Biosciences	563220	2 µg/mL	
CD3e-PECy7	BD Biosciences	552774	2 µg/mL	
CD4-FITC	BD Biosciences	561835	2.5 µg/mL	
Podoplanin-PE	Angiobio	11-009PE	1:100 dilution	
CD41	Biolegend	133910	25 µg/mL	
Lyve1	Angiobio	11-034	0.5 µg / slide	
CD41	Abcam	ab134131	1:1000 dilution	
TSG-101	Abcam	ab83	1:666 dilution	

Cultured Cells

Name	Vendor or Source	Sex (F, M, or unknown)
HMVEC-dLyAd	Lonza CC-2810	F